Available online at www.sciencedirect.com

SCIENCE DIRECT

Biochimica et Biophysica Acta 1669 (2005) 193–207

BIOCHIMICA ET BIOPHYSICA ACTA
BBA

http://www.elsevier.com/locate/bba

New effects in polynucleotide release from cationic lipid carriers revealed by confocal imaging, fluorescence cross-correlation spectroscopy and single particle tracking

Svitlana Berezhna[a,*], Stephan Schaefer[b], Rainer Heintzmann[a], Michael Jahnz[b], Guido Boese[a], Ashok Deniz[c], Petra Schwille[b]

[a]*Max Planck Institute for Biophysical Chemistry, Am Fassberg 11, 37077 Goettingen, Germany*
[b]*Institute of Biophysics/Biotec, Dresden University of Technology, Tatzberg 47-51, 01307 Dresden, Germany*
[c]*The Scripps Research Institute, Department of Molecular Biology, 10550 North Torrey Pines Road, MB-19, La Jolla, CA 92037, USA*

Received 14 September 2004; received in revised form 9 February 2005; accepted 9 February 2005
Available online 10 March 2005

Abstract

We report on new insights into the mechanisms of short single and double stranded oligonucleotide release from cationic lipid complexes (lipoplexes), used in gene therapy. Specifically, we modeled endosomal membranes using giant unilamellar vesicles and investigated the roles of various individual cellular phospholipids in interaction with lipoplexes. Our approach uses a combination of confocal imaging, fluorescence cross-correlation spectroscopy and single particle tracking, revealing several new aspects of the release: (a) phosphatidylserine and phosphatidylethanolamine are equally active in disassembling lipoplexes, while phosphatidylcholine and sphingomyelin are inert; (b) in contrast to earlier findings, phosphatidylethanolamine alone, in the absence of anionic phosphatidylserine triggers extensive release; (c) a double-stranded DNA structure remains well preserved after release; (d) lipoplexes exhibited preferential binding to transient lipid domains, which appear at the onset of lipoplex attachment to originally uniform membranes and vanish after initiation of polynucleotide release. The latter effect is likely related to phosphatidyleserine redistribution in membranes due to lipoplex binding. Real time tracking of single DOTAP/DOPE and DOTAP/DOPC lipoplexes showed that both particles remained compact and associated with membranes up to 1–2 min before fusion, indicating that a more complex mechanism, different from suggested earlier rapid fusion, promotes more efficient transfection by DOTAP/DOPE complexes.

Keywords: Lipoplex; Endosomal membrane; Release mechanism; Giant unilamellar vesicles; Fluorescence microscopy; Single particle tracking

1. Introduction

Following decades of extensive research, lipid-based delivery systems have entered the mainstream as carriers of nucleic acids, either for plasmid delivery or as agents for carrying short antisense single strand oligonucleotides (ODN) to express or to down-regulate target genes in therapeutic applications. With many of the early problems related to carrier toxicity, biodegradability and stability recently ameliorated, a notorious drawback of the lipid-based vehicles remains poor efficiency [1–7].

Formation of the lipoplexes and their interaction with cellular components, leading to intracellular access of the

Abbreviations: GUVs, giant unilamellar vesicles; PS, phosphatidylserine; PE, phosphatidylethanolamine; PC, phosphatidylcholine; SM, sphingomyelin; DOTAP, dioleoyltrimethylammonium propane; DOPE, di-oleoyl phosphatidylethanolamine; DOPC, di-oleoyl phosphatidylcholine; DPPS, di-palmitoyl phosphatidylserine; DOPS, 1,2-dioleoyl-*sn*-glycero-3-phospho-L-serine; DiO, 3,3′-dihexadecyloxacarbocyanine perchlorate ($DiOC_{16}$ (3)); ITO, indium tin oxide; HPLC, high performance liquid chromatography; LSM, laser scanning confocal fluorescence microscopy; FCCS, fluorescence cross-correlation spectroscopy; SPT, single particle tracking; PCR, polymerase chain reaction

* Corresponding author. Present Address: The Scripps Research Institute, Department of Molecular Biology, 10550 North Torrey, Pines Road, MB-19, La Jolla, CA 92037, USA. Tel.: +1 858 784 2911; fax: +1 858 784 9067.
E-mail address: berezhna@scripps.edu (S. Berezhna).

0005-2736/$ - see front matter © 2005 Elsevier B.V. All rights reserved.
doi:10.1016/j.bbamem.2005.02.011

carrier, lipoplex disassembly and polynucleotide release into cell cytosol have been extensively investigated using various techniques [6–28], aiming to determine a composition–structure–function relationship and to develop a rationalized approach in designing efficient carriers. It has been proposed that the delivery potential of the carrier is determined by the internal nano-structure of the complex [12,13,16,19], its total surface charge [10,11,14] along with lipid charge density [21]. However, it remains to be fully understood how the lipoplexes are disassembled as they are taken up by cells, and by what mechanisms and to what degree (fully or not) DNA/ODN dissociate from the carrier lipids during this process.

At present, it is widely accepted that lipoplexes enter cells via endocytosis [23–28]. To carry out its function, DNA has to escape from endosomal compartments while simultaneously detaching itself from the carrier lipids and be released into the cytosol—a complex mission, whose fate and driving mechanisms are not fully understood. Considering that phospholipid content is an important factor in determining biophysical properties of the membranes [29,30], understanding phospholipid roles in interaction with the lipoplexes has been highly significant for uncovering release mechanisms. Indeed, phospholipids have been regarded as major species involved in interaction with the lipoplexes [26,31–33], while cholesterol showed no effect on DNA/ODN release [32]. A current understanding of the release mechanism, as suggested by Szoka et al [26,31,32], proposes that due to interaction with the lipoplexes, anionic phospholipids from the cytoplasmic-facing leaflet of the endosomal membrane enter into its internal leaflet, resulting in the formation of a charge-neutral ion pair between anionic cellular lipids (phosphatidylserine, PS) and cationic lipids. Such a coupling of anionic PS to cationic lipids leads to DNA displacement from the complex and release, due to electrostatic forces. In fact, it has long been postulated that perturbation of lipid asymmetry in the membrane bilayer, involving transmembrane re-distribution of aminophospholipids (PS and phosphatidylethanolamine, PE) in endosomal membranes, is a general aspect of endocytosis [34–37]. Recent experimental studies have given new evidence for this hypothesis, generally pointing toward a more active role of lipid re-arrangement in inducing membrane invagination during endocytosis [38–41]. Still, it remains questionable whether energy costly lipid flip-flop, which would require several hours [42], can happen within the time scale of a continuous endocytosis process, and whether the cationic complexes can be promoters of trans-leaflet lipid mixing in the endosomal membranes. Also, the exact role of cellular PE lipid along with usage PE as a “helper” lipid in cationic complexes remain intriguing and need better understanding [43–47].

In this work, we model endosomal membranes by giant unilamellar vesicles (GUV) and investigate the distinct roles of major cellular phospholipids (PC, PE, PS and sphingomyelin, SM) in interaction with the cationic lipid-DNA/ODN complexes, aiming to gain a deeper insight into the release mechanisms. In contrast with small liposomes, used in the previous studies, the GUV system not only allows visualization of the release process, but also investigation of the state of the target membrane during and after the interaction with lipoplexes. We examine the extent of release of short single and double stranded DNA across model membranes by laser scanning confocal imaging. Also, we use fluorescence cross-correlation analysis of DNA diffusion to assess whether DNA has been detached from the carrier lipids and if the double-stranded DNA has dissociated into single strands upon release. In addition, we apply single particle tracking methodology to monitor in real time and at the level of single lipoplexes the course of lipoplex fusion with the membranes. The observed effects are discussed in the context of interactions between cationic lipid-DNA/ODN complexes and cellular membrane lipids.

2. Materials and methods

2.1. Materials

Lipids included cationic DOTAP (dioleoyl-trimethylammoniumpropane), anionic DPPS (dipalmitoyl-phosphatidylserine), DOPS (1,2-dioleoyl-sn-glycero-3-phospho-L-serine) and neutral DOPE (dioleoyl-phosphatidylethanolamine), DOPC (dioleoyl-phosphatidylcholine), SM (sphingomyelin). All lipids were purchased from Avanti Polar Lipids (Alabaster, AL). The lipid analog fluorescent dye 3,3′-dihexadecyloxacarbocyanine perchlorate (DiO) was received from Molecular Probes (Eugene, Oregon).

A 66-nt single strand oligonucleotide with the sequence as described elsewhere [48] was labeled at its 5′ end with Alexa 488 and its complementary strand with Cy-5. They were annealed by the standard procedure to obtain a 66-nt double-stranded double-labeled (Alexa 488 and Cy-5 at the ends) DNA. Double-stranded 368-nt DNA labeled with Cy-5 at the 5′-end was generated by PCR using TaKaRa Ex Taq Polymerase. All oligonucleotides were custom synthesized, HPLC purified and labeled by IBA GmbH. (Goettingen, Germany). PCR reaction products (1 ml) were purified and concentrated using the MiniElute PCR-Purification Kit (Qiagen, Hilden, Germany). Further purification was done by extraction from 1.5% (w/v) agarose gel (NucleoSpin extract, Macherey and Nagel GmbH, Duren, Germany) and ethanol precipitation. DNA was dissolved in LichroSolv HPLC water (Merck, Darmstadt, Germany) at a final concentration of ~100 nM. Note, henceforward to clarify what type of oligonucletotide is discussed in the specific experiments we additionally specify ss-ODN or ds-DNA when relevant.

2.2. Preparation of liposomes and lipoplexes

Chloroform solutions of lipids (DOTAP/DOPE and DOTAP/DOPC at various mole fractions) were dried under

nitrogen stream followed by the removal of residual solvent under vacuum for ~2 h. Lipid films were hydrated in 1 ml of HPLC grade water. To form uniform small unilamellar vesicles, liposome solutions were vortexed for several minutes and passed 11 times through a mini-extruder (Avanti Polar Lipids, Alabaster, AL) using two 100 nm pore-size polycarbonate filters. All preparations were extruded at temperatures above the gel-to-liquid crystalline phase transition. The final preparations were stored at 4 °C under argon atmosphere until use.

Using appropriate amounts of liposome and DNA/ODN stock solutions doped with a desired concentration of fluorescent DNA/ODN molecules, lipoplexes were prepared at a cationic-to-anionic charge ratio 3:1 in HPLC water (20 μl total solution volume) by adding equal volume of DNA/ODN solution into liposomes, gentle mixing and incubating for 20 min at room temperature. The preparation was diluted to a final volume of 380 μl in HPLC water or in PBS buffer and injected into the side channel of the 400 μl flow chamber containing the GUV sample. In the experiments with lipoplexes diluted in PBS buffer, before injection of lipoplex solution, the GUV sample was flushed with PBS buffer by gentle injection of 400 μl of the buffer into the chamber. Amounts of labeled DNA/ODN molecules in the lipoplex preparations were 100 pmol for LSM experiments, and in the range of 1–10 pmol for FCS and SPT measurements, respectively.

2.3. Preparation of GUVs

GUVs were prepared using 5 mM stock solutions of corresponding lipid mixtures in chloroform or chloroform/methanol (in the case of PS) by using an electro-formation method with indium tin oxide (ITO) coated cover-slips [49,50]. This technique was proven to yield a high percentage of unilamellar vesicles with negligible lipid oxidation [49–51]. GUVs were formed in a water medium using a specially designed flow chamber; a sinusoidal voltage of 1.2 V amplitude at 10 Hz was applied to the ITO cover-slips for ~1 h at 60 °C. If needed for visualization in the LSM experiments, 0.1 mole% of DiO lipid analog dye was added to each lipid mixture.

2.4. Laser scanning confocal fluorescence imaging of DNA/ODN release

LSM confocal imaging was used to visualize the interaction of lipoplexes with giant vesicles, and to estimate the extent of DNA release from the lipoplexes for various membrane lipid formulations. LSM imaging was performed on a Zeiss 510 laser scanning microscope (Zeiss, Jena, Germany) in the epi-detection configuration using a water immersion objective 40×/1.2 W, (Zeiss, Jena, Germany) with an adjustable pinhole at 76 μm. For fluorescence excitation, Ar ion (used at 488 nm, 30 mW,) and He–Ne (633 nm, 5.0 mW) lasers were used at 10% of maximum output and at full power, respectively. A combination of a band-pass filter transmitting 505–550 nm (Zeiss, Jena, Germany) and a long pass filter at 650 nm (Zeiss, Jena, Germany) was applied to separate DiO (and/or Alexa 488) and Cy-5 fluorescence.

The extent of DNA release was evaluated based on monitoring the release-induced buildup of a concentration gradient of fluorescently labeled DNA inside the GUVs. GUV membranes were visualized by adding DiO fluorescent dye, while lipoplexes contained DNA, labeled either with Cy-5 or Alexa 488 fluorophore, or both. Initially, GUVs are void of DNA; after lipoplex injection, a certain fraction of vesicles eventually accumulate DNA inside. After 2 h, we collect a set of images for randomly chosen sample regions and determine the extent of DNA release. A number of images for the given sample was acquired such that, in total, the set contains ~300 vesicles. The experiments were always carried out using the same excitation intensity in the sample, and the same amplification settings for the detectors. The excitation intensity was adjusted such that it provides sufficient fluorescent signal of released DNA inside vesicles, but avoids fast fluorophore photobleaching. The samples were injected with the lipoplexes, containing the same amount of labeled DNA molecules. A vesicle was counted as DNA-filled, when the average fluorescence signal throughout the vesicle lumen, measured in the corresponding channel (red or green, depending on the fluorescent label on DNA) was equal to or higher than a pre-fixed threshold value (100 ADU over the background). This value was determined based on preliminary analysis of multiple samples with varying membrane lipid composition. Data processing included applying a corresponding intensity threshold to the image, which allows us to select only DNA-filled GUVs. Although not quantitatively exact for absolute estimation of DNA release, this criterion allowed for a relative comparison of DNA release and provided a basis for statistical analysis. The extent of DNA release from the lipoplexes was evaluated here as a percentage of DNA-filled vesicles versus the total number of vesicles (~300) in the selected sets of images. For data averaging, each specific experiment was repeated 4 times, corresponding to the evaluation of approximately 1200 vesicles for every lipid mixture.

A series of negative controls was carried out to verify the permeability/stability of the vesicles to: (a) free labeled-DNA/ODN (not enveloped in lipid coating); (b) free, fluorescent dye molecules (not attached to DNA). The data, obtained in the control experiments (several corresponding images are given in Results Section) showed that after 5 h of incubation with free labeled ds-DNA or ss-ODN (carrying either Alexa 488 or Cy-5, or both fluorophores) the fraction of leaky vesicles in the sample was less than 5% (the vesicles, which were filled with labeled probes due to probe diffusion across defective membrane). Similar results were obtained for free Alexa-488 fluorophore. In contrast to the

active transport of DNA inside vesicle lumen due to lipoplex interaction with target membrane, a steep increase of labeled DNA concentration inside the GUV lumen versus the outside solution was never built up by free diffusion of DNA into leaky vesicles. For the lipoplex formulations used here, a fraction of free labeled DNA molecules available in the solution after formation of the complexes was undetectable in LSM images. Therefore, the effect of the small proportion of leaky vesicles on quantifying DNA-filled GUVs was negligible because leaky vesicles were discarded during applying the intensity threshold. It is possible that while the lipoplexes interact with the target membrane and DNA dissociate from the carriers, the release may occur on both sides of the membrane with a certain fraction of nucleotide releasing not into the vesicle lumen, but into the outside medium. However, this does not influence our investigations of release process as the amount of molecules released "outside" was not observable in bulk medium in LSM images.

In some experiments, injection of lipoplex solution into the sample caused GUVs to move, which either resulted in a stabilized pattern later on or not. In the latter case the sample was discarded. Other than the vesicle movement in response to lipoplex injection, we did not observe any image blurring due to thermal motion or other factors at the scanning speed used.

2.5. Fluorescence cross-correlation analysis of DNA diffusion

Dual-color fluorescence cross-correlation analysis of DNA diffusion is applied here to evaluate a fraction of double-labeled, ds-DNA species inside giant vesicles after the DNA is released from the cationic complexes, which were prepared using originally double-labeled, double-strand DNA. The FCCS measurements were performed on a commercial setup ConfoCor2 (Zeiss, Jena, Germany). An Ar ion laser at 488 nm and a He–Ne laser at 633 nm were used for excitation of Alexa 488 and Cy-5 fluorescence, respectively. The microscope was used in the epi-detection configuration, with a Zeiss C-Apochromat 40×/1.2 W water immersion objective. The fluorescence emission was split by a dichroic mirror (NFT 545) into the two channels and additionally filtered by passing respectively through the 505–550 band-pass and 650 long pass filters (Zeiss, Jena, Germany). Avalanche photodiodes (Perkin Elmer, Optoelectronics, Vaudreuil, Canada) were used for detection. Confocal geometry was provided by applying a pinhole (90 μm) in front of the detector. The laser focus was positioned inside the vesicle by performing an in-plane (XY-) and axial (Z-) scanning through the vesicle. Auto- and cross-correlation analysis of DNA diffusion were performed according to procedures described in detail elsewhere [51]. Experimentally obtained correlation functions were numerically fitted by the Levenberg–Marquardt nonlinear least-squares algorithm (ORIGIN, OriginLab, Northampton, MA) using the following equations:

$$G_{gg}(\tau) = \frac{<C_g>Diff_g(\tau) + <C_{gr}>Diff_{gr}(\tau)}{V_{eff}\left(<C_g> + <C_{gr}>\right)^2} \quad (1a)$$

$$G_{rr}(\tau) = \frac{<C_r>Diff_g(\tau) + <C_{gr}>Diff_{gr}(\tau)}{V_{eff}\left(<C_r> + <C_{gr}>\right)^2} \quad (1b)$$

$$G_{gr}(\tau) = \frac{<C_{gr}>Diff_{gr}(\tau)}{V_{eff}\left(<C_g> + <C_{gr}>\right)\left(<C_r> + <C_{gr}>\right)}, \quad (1c)$$

where

$$Diff_{i=g,r,gr}(\tau) \equiv \left(1 + \tau/\tau_{d,i}\right)^{-1}\left(1 + r_0^2\tau/z_0^2\tau_{d,i}\right)^{-1/2}$$

denotes the temporal decay of either correlation function due to molecular diffusion of species i with a diffusion time of $\tau_{d,i}\cdot C_g$, C_r and C_{gr} are concentrations of green, red and green-red fluorescent molecules, respectively. The parameters r_0 and z_0, describing the excitation volume in lateral and axial directions, respectively, are determined by the experimental geometry and V_{eff} is the effective measurement volume.

2.6. Monitoring lipoplex fusion by single particle tracking

The setup was assembled in a wide field epifluorescence configuration using an Olympus IX-50 microscope with 60×/1.20 W UPlanApo water immersion objective (Olympus), equipped with a sensitive fast-frame CCD camera (CoolSnap HQ, Roper Scientific Co., USA, a 1392 × 1040 pixel chip, pixel size 6.45 × 6.45 μm^2) and an acousto-optic modulator (AA.MOD.4C, A.A. Sa Co.). For illumination, an Ar/Kr ion laser (Innova 70, Coherent) was used at 488 or 647 nm. Image acquisition was performed using commercial software (WinSpec/32, Roper Scientific Co.). The illumination time was 10 ms per frame, with 40 ms lag time between two consecutive images. The obtained image sequences were processed and analyzed by in-house software (C++) to extract the x- and y-coordinates of the particles over time and to reconstruct particle trajectories. The particles were identified by the user in the image of their first appearance. In every subsequent image, the tracking algorithm followed the particle by iteratively updating the local maximum (in a 5 × 5 pixel neighborhood search region) starting with the particle position in the previous time-frame. The algorithm then places a 5 × 5 pixel kernel around this local maximum and evaluates the centroid of the intensity in this region after subtraction of the minimum intensity of this region (calculating the center of mass of the "cap"), which gives particle coordinates. This procedure allowed us to trace a particle automatically, unless the tracked particle came close to the other particles within a 5 × 5 pixel kernel, which was verified by the user. Also, if a particle vanished before the last frame in the sequence, its

trace was stopped at its last visible position by user interaction. On average, 20–30 particles were tracked for each specific experiment, described in Section 3 (Results). The same experiment was repeated 3 times, corresponding to evaluation of approximately 60–90 particles in total for the given type of experiment. The localization accuracy, as estimated according to a procedure described earlier [52], was ~20 nm or better, depending on the signal-to-noise ratio.

3. Results

Probing interaction of lipoplexes with an individual molecular species in intact cell membranes of living cells is hard to achieve. Therefore, this process is studied here in a simplified context using a protein-free membrane assay of giant unilamellar vesicles (GUVs). Artificial membranes do not reproduce the entire complexity of real biological membranes. However, they do provide a relevant model for investigating membrane fusion inasmuch as this process refers to the lipid bilayers [41]. Until now, lipoplex interactions with membranes in vitro were investigated using large unilamellar vesicles. Several previous assays were based on adding liposomes to a solution of fluorescently labeled lipid-DNA/ODN complexes and evaluating complex disruption by monitoring quenching or appearing of the fluorescence signal of a certain compound, which signifies fusion of liposomes with the cationic lipids and DNA/ODN release [26,31,32,43,44,53]. The uniqueness of the new assay used here is that giant liposomes allow us to directly visualize the course of lipoplex binding to the membranes, fusion, DNA release and to monitor the state of the contacting membrane.

Phosphatidylcholine (PC), phosphatidylethanolamine (PE) and phosphatidylserine (PS) are major phospholipids of the endosomal membranes [29,30]. On average, their contents are, respectively, around 55%, 25% and 10–15% of total phospholipids [29,30,58]. Taken together, these lipids typically constitute approximately 90% of entire phospholipids, with the other common membrane phospholipid sphingomyelin (SM) presenting about 10%, and the rest are small amounts of phosphatidylinositol and cardiolipin [29]. Therefore, to mimic lipid formulation of the endosomal membranes, we prepared GUV using PS, PE, SM and PC in the molar fractions 0.1/0.25/0.1/0.55, respectively. In other formulations, SM was excluded and we used only PS, PE and PC in the amounts 0.15/0.25/0.6, respectively. Further, PS was excluded in addition to SM, and we probed lipid formulations of 0.25/0.6 and 0.4/0.6 PE/PC. Next, PS was probed in composition with PC at 0.15/0.85 and 0.25/0.75 fractions. Finally, we examined pure PC membranes. In all studied lipid formulations, PE and PC lipids were used as unsaturated species, dioleoyl-phosphatidyl-ethanolamine (DOPE) and DOPC, respectively, while PS was used both as dipalmitoyl-phosphatidylserine (DPPS) and as 1,2-dioleoyl-sn-glycero-3- phospho-L-serine (DOPS). This replicates the distribution of saturated and unsaturated molecular species for these specific types of lipids as found in cells [29,54]. Using PS in two different modifications also provides a possibility to estimate the influence of the acyl group of PS on effectiveness of polynucleotide release. Table 1 provides the entire list of membrane formulations investigated here.

3.1. Confocal imaging of polynucleotide release from lipoplexes

Fig. 1 shows images of a freshly prepared GUV sample (A, B) along with results of negative controls with injection of free labeled ds-DNA and ss-ODN (C, D). The images in Fig. 1 were obtained for DOPS/DOPE/DOPC (0.15/0.25/0.6) GUVs labeled with 0.1 mol% of DiO, and provide a typical example of the sample with respect to vesicles shape, size scatter and spatial distribution. Initially, all vesicles are empty, except for the medium inside (Fig. 1A). Fig. 1B gives a representative three-dimensional projection of the vesicles, reconstructed from a series of the confocal slices. Partitioning of DiO dye into a certain lipid phase has been shown to clearly visualize formation of lipids domains in the giant vesicles [51,55]. Fig. 1A, B evidence that constituent lipid species homogeneously dispersed in the bilayers, showing no formation of macroscopic lipids domains. Injection of free ds-DNA or ss-ODN molecules shows no visible polynucleotide transfer across the GUV membranes during long observation time (over 5 h) as seen in Fig. 1C (double-labeled 66-nt ds-DNA) and Fig. 1D (single-labeled 66-nt ss-ODN). In general, less than 5% of GUVs in the samples were permeable to free ds-DNA and/or ss-ODN molecules in the control experiments for each lipid composition.

In contrast with free polynucleotides, lipoplex addition to the sample results in dynamic binding of the lipoplexes to the GUVs surfaces. Eventually, interaction between the

Table 1
Extent of ODN release from DOTAP/DOPE lipoplexes (0.5/0.5 lipid molar fractions, 3:1 cationic lipid/anionic ODN charge) for different membrane compositions

Membrane formulation	Lipid content in molar fraction	Extent of DNA release (% of DNA-filled GUVs; mean of 4 experiments, ±2%)
DOPS/DOPE/SM/DOPC	0.1/0.25/0.1/0.55	33%
DPPS/DOPE/SM/DOPC	0.1/0.25/0.1/0.55	35%
DOPS/DOPE/DOPC	0.15/0.25/0.6	38%
DPPS/DOPE/DOPC	0.15/0.25/0.6	36%
DOPS/DOPC	0.15/0.85	10%
DPPS/DOPC	0.15/0.85	12%
DOPS/DOPC	0.25/0.75	22%
DPPS/DOPC	0.25/0.75	20%
DOPE/DOPC	0.25/0.75	25%
DOPE/DOPC	0.4/0.6	35%
DOPC	1	5%

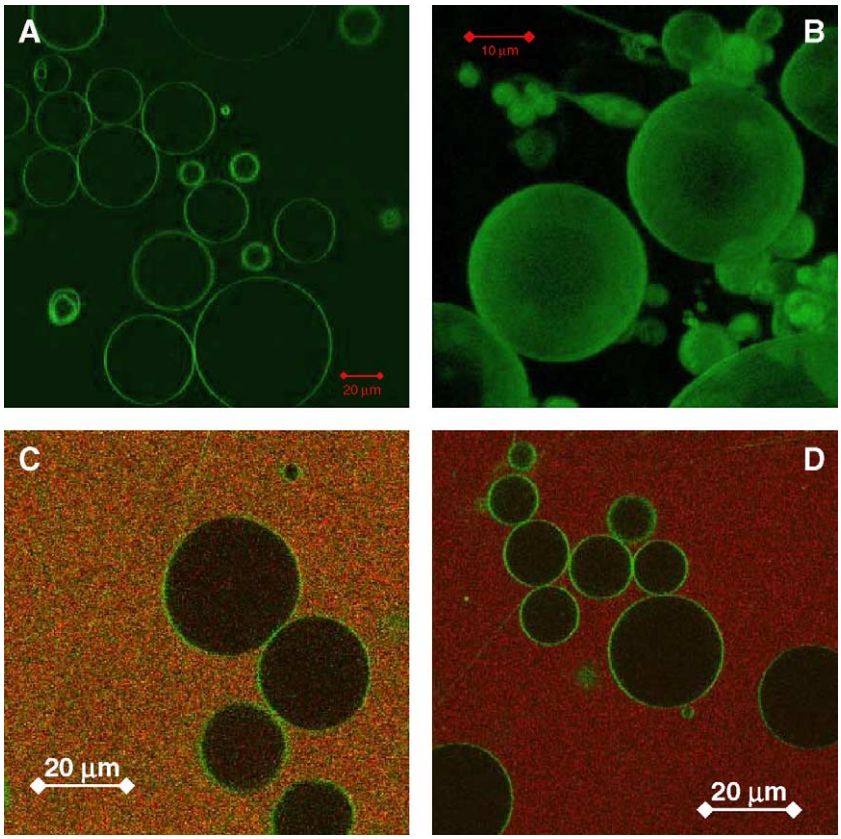

Fig. 1. Laser scanning confocal microscopy images of DPPS/DOPE/DOPC (0.15/0.25/0.6) GUVs, labeled with 0.1 mol% of DiO (green color). (A) a confocal image (~0.7 μm thick) showing the freshly prepared GUV sample; (B) a three-dimensional projection, reconstructed from a series of the subsequent confocal slices (0.7 μm thick) using the Zeiss imaging software of ConfoCor2; (C) a confocal image of the GUV sample, taken ~5 h after injection of 100 pmol of double-labeled DNA (each of the two complementary 66-nt oligonucleotides carries fluorescent dyes Cy-5 and Alexa 488, respectively, visible together in yellow color); (D) a confocal image of the sample at ~3 h after the injection of 100 pmol of Cy-5 labeled ODN (66-nt single strand, visible in red color).

complexes and the membrane results in the creation of a visible concentration gradient of DNA inside the vesicles. The images in Fig. 2 show a DOPS/DOPE/DOPC (0.15/0.25/0.6) GUV sample approximately 30 min after injection of DOTAP/DOPC-.15 ODN complexes (DOTAP/DOPC at 0.9/0.1 mole fraction, 66-nt Cy-5 labeled ss-ODN). Fig. 2A shows the "red" channel, Fig. 2B the "green" channel, and Fig. 2C shows the overlay of both channels. As clearly seen in Fig. 2B, lipoplex binding to the membrane induces extensive vesiculation (budding) of the lipid bilayer with formation of numerous sprouting vesicles; the effect was not observed in the absence of the lipoplexes. Membrane vesiculation in response to lipoplex binding was, in general, seen for all lipid formulation studied here. At the same time, formation of such budding vesicles was less expressed for a pure DOPC membrane, while an increase of DOPE amount in the membrane tends to enhance this effect.

To quantify the effect of the membrane lipid content on the extent of polynucleotide release, we determined the percentage of filled vesicles in the sample 2 h after injecting the lipoplexes. In all cases, the samples were injected with the same amount of analogous lipoplexes (DOTAP/DOPE at 0.5/0.5 fractions, 3:1 charge ratio, 100 pmol of 66-nt Cy-5 labeled ss-ODN). The maximum efficiency of DNA release was observed for DOPS/DOPE/DOPC and DPPS/DOPE/DOPC membrane lipid formulations, approximately ~38% ± 2%. For the lipid formulations with lowered fraction of PS and added SM (DOPS/DOPE/SM/DOPC and DPPS/DOPE/SM/DOPC), the extent of release remained the same and again, did not differ for DOPS and DPPS containing mixtures, ~35% ± 2%. In the formulations, containing only the two lipids, PC and anionic PS, the percentage of filled vesicles increased with the increase of fraction of PS. For the double formulation of PC and neutral PE the same tendency was observed with the elevated release for higher PE fraction. Pure DOPC membranes showed very low degree of release (the number of filled vesicles was ~5%). Additionally, for several lipid formulations, showing the highest (DOPS/DOPE/DOPC, DOPE/DOPC) and lowest (DOPC) activity, respectively, we investigated polynucleotide release using lipoplexes prepared from 66-nt ds-DNA and 368-nt ds-DNA. We determined no significant difference in the ratio of polynucleotide-filled vesicles in these measurements, and the level of DNA release remained at ~35% for DOPS/DOPE/DOPC and at ~5% for DOPE membranes, respectively. All data are the averages of 4 experiments; the standard deviation is ± 2%.

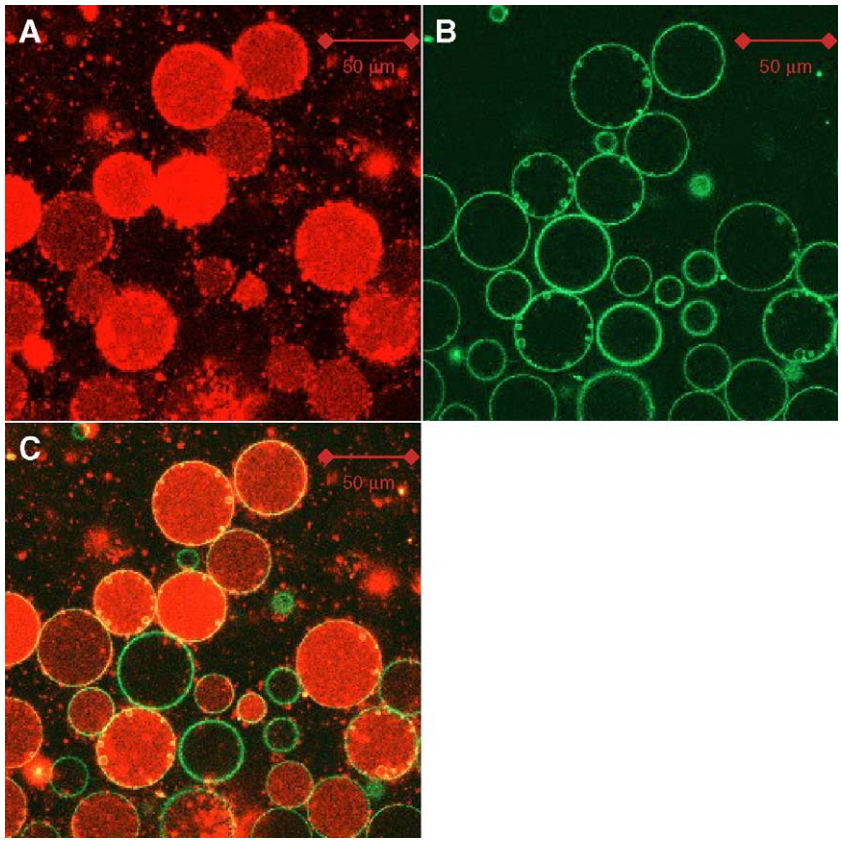

Fig. 2. Laser scanning confocal microscopy images of DOPS/DOPE/DOPC (0.15/0.25/0.6) GUVs, labeled with 0.1 mol% of DiO (green color), acquired approximately 30 min after injecting DOTAP/DOPC–DNA complexes (DOTAP/DOPC at 0.9/0.1 lipid mole fraction). 66-nt Cy-5 labeled ODN is seen by red color fluorescence when released inside GUVs. (A) a confocal image in the red channel; (B) a confocal image in the green channel; (C) overlay of the images from the both channels.

To verify the role of external medium ionic condition on the release, the experiments were also repeated for DOPS/DOPE/DOPC membrane (showing a high level of nucleotide release) in PBS buffer. We did not observe a change of DNA release in PBS buffer as compared to water medium (~35%). This result is in agreement with the earlier studies of DNA release from lipoplexes as function of various pH and ionic conditions by others [32].

3.2. Transient domain formation in anionic GUVs due to lipoplex binding

Following lipoplex injection, GUVs were typically seen to immediately accumulate the fluorescently labeled particles on their surfaces. The complexes were binding the membranes at random, and were visible as red or yellow dots evenly distributed along the vesicle's rim in the confocal images. After approximately 15 min, some vesicles started to build up an observable concentration gradient of released polynucleotides, emerging as disperse fluorescence pattern within the vesicle lumen. At the same time, other vesicles continued to accumulate the fluorescent particles exclusively on their surface, showing no released DNA inside. After approximately 30 min, a certain number of the vesicles (depending on the composition of the membrane) were filled with labeled polynucleotides. Usually, such DNA-filled vesicles did not display a noticeable pattern of the bound particles on their surfaces, and their membranes were seen as clear green circles, limiting diffuse red fluorescence inside. On the other hand, other vesicles failed to accumulate polynucleotides inside, and were seen as empty circles but abundantly covered with the fluorescent particles all around their outer surfaces. On average, 1 h after injection of the complexes a reasonably stabilized pattern of DNA/ODN-filled and empty vesicles was formed in the sample. In control experiments, the number of polynucleotide-filled vesicles did not change significantly after the sample was left to interact with the complexes for additional 3 h. The observations were common to all studied lipid formulations, except for the membrane compositions, containing PS lipids.

An interesting effect was observed at an early step of lipoplexes interaction with the GUVs, containing PS. After lipoplexes were added to the sample and diffused to the GUV surfaces, the GUVs clearly displayed a pattern of uneven, patch-like lipoplex binding. Instead of the above described uniform distribution of the lipoplexes on the vesicle's rim, they were tending to bind to the membrane at specific sites, where other lipoplexes were already seen

attached. This resulted in creating a transient pattern of preferential binding domains, appearing on the vesicle surfaces for short time intervals, as demonstrated in Fig. 3. Clearly, such "binding-keen" domains were created in the vesicle membranes randomly depending on the site, where a few first complexes approached the surface. Eventually, the "patchy" vesicles either started to accumulate released polynucleotide inside, or remained void, but continued to collect bound complexes amply on their surfaces. In either case, the early seen domains dispersed when a larger amount of the lipoplexes attached to the membrane. Typically, the domain pattern was observable in the vesicle for several minutes, following lipoplex addition. The appearance of the domain structure was frequent for the vesicles with lipid compositions containing either DPPS or DOPS (both for DOTAP/DOPE-and DOTAP/DOPC lipoplexes), but was never observed for other membrane formulations. However, quantitative estimation of the number of vesicles with preferential complex binding patterns was not possible due to the transient state of this phenomenon.

3.3. DNA release from DOTAP/DOPE and DOTAP/DOPC lipoplexes

To look into the effect of the "helper" lipid content on the level of polynucleotide release from DOTAP based lipoplexes, we varied both the type (DOPE or DOPC) and the molar fraction of the "helper" lipids, and injected the obtained series of lipoplexes to DOPS/DOPE/DOPC vesicles. Both DOTAP/DOPE and DOTAP/DOPC lipoplexes were destabilized during interaction with the given membrane and released polynucleotides inside GUVs. However, the level of DNA dissociation from DOTAP/DOPC complexes decreased, from about ~35% to ~5%, with the increase of DOPC amount in the lipoplex from 0.1 to 0.9 molar fraction (Fig. 4). For DOTAP/DOPE-ODN complexes, the extent of ODN release from the lipoplexes was significant (~35%) and independent of the amount of DOPE in the lipoplex (Fig. 4). Additionally, we injected DOTAP/DOPC lipoplexes at 0.1 molar fraction of DOPC to the vesicles devoid of PS, DOPE/DOPC at 0.25/0.75 and observed a considerable level of the release, ~20%.

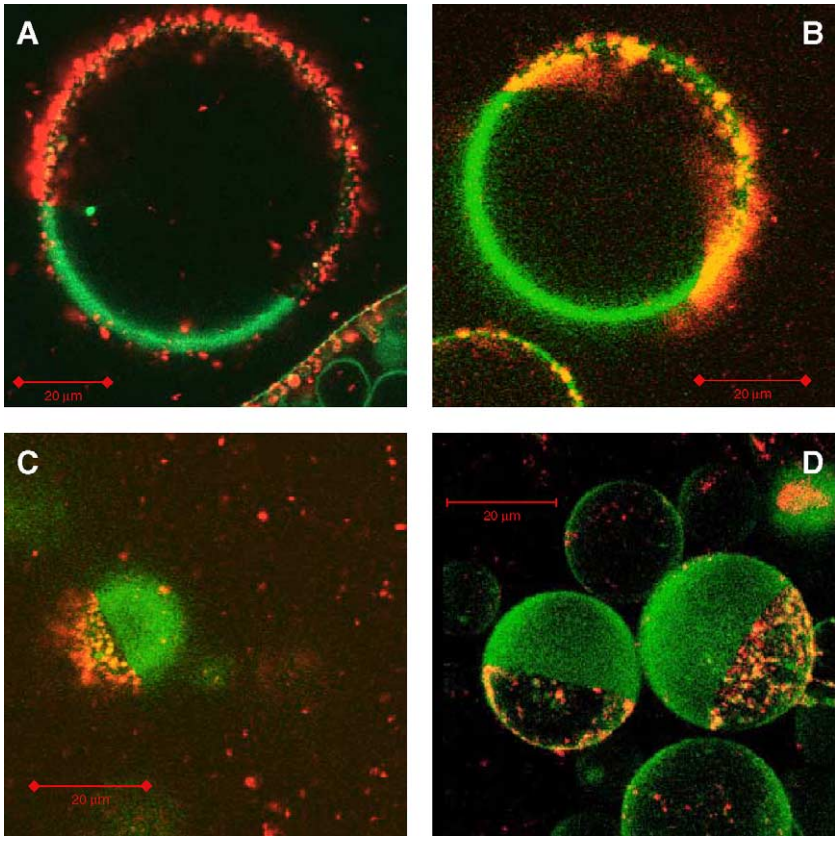

Fig. 3. Laser scanning confocal microscopy images of PS/DOPE/DOPC (0.15/0.25/0.6) GUVs labeled with 0.1 mol% of DiO (green color), demonstrating transient patterns of preferential lipoplex binding. (A) a confocal image of DOPS/DOPE/DOPC GUVs sample, approximately 5 min after injection of DOTAP/DOPC lipoplexes (at 0.9/0.1 mole fraction of cationic lipid to helper lipid); (B) a confocal image of DPPS/DOPE/DOPC GUVs sample, about 7 min after adding DOTAP/DOPE lipoplexes (at 0.5/0.5 lipid mole fraction); (C) a confocal image of DOPS/DOPE/DOPC GUV close to the vesicle top ~10 min after injecting DOTAP/DOPE lipoplexes (at 0.3/0.7 lipid mole fraction); (D) a three-dimensional projection, reconstructed from the series of the confocal slices (0.7 μm thick) using the Zeiss imaging software of ConfoCor2 for DPPS/DOPE/DOPC sample, injected with DOTAP/DOPE lipoplexes (at 0.7/0.3 lipid mole fraction), ~10 min after injection. In all experiments the lipoplexes were prepared using 66-nt Cy-5 labeled ODN.

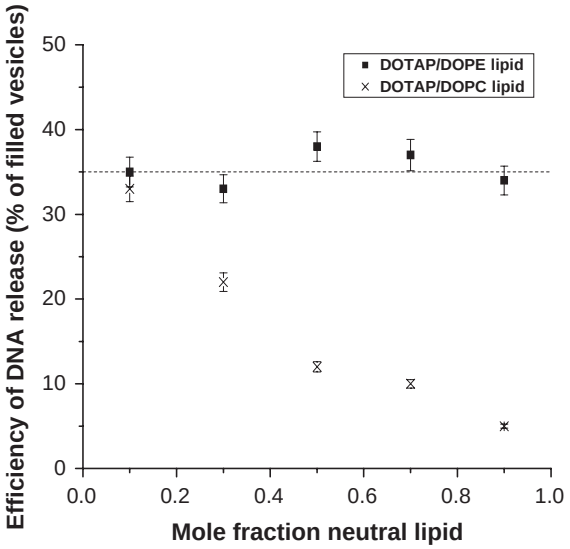

Fig. 4. Extent of polynucleotide release from the various lipoplexes during interaction with DOPS/DOPE/DOPC (0.15/0.25/0.6) membrane. Each data point is a result of averaging 4 independent measurements. The lipoplexes were prepared at a fixed cationic/anionic charge ratio 3:1 using 66-nt Cy-5 labeled ODN and DOTAP/DOPE or DOTAP/DOPC liposomes in the mole fractions of cationic to helper lipids as given in the plot.

3.4. Fluorescence cross-correlation analysis of DNA diffusion

In the confocal imaging experiments, we observed that when double-labeled ds-DNA carrying a different label on each of complementary strands, is released from the lipoplexes, the DNA-filled vesicles exhibit simultaneously red and green fluorescence inside. Single color vesicles were not visible. This provides likely evidence that the DNA remains double-stranded. To examine this observation in quantitative terms, we applied fluorescence cross-correlation spectroscopy to measure and analyze DNA diffusion. FCCS, recognized by its ability to quantify molecular interactions and diffusion with high precision [52,56], provides a sensitive tool to evaluate the relative amount of double-labeled, double-stranded DNA species diffusing in a solution by measuring a cross-correlation function of red and green fluorescence signals. The amplitude G(0) (time-zero value) of the cross-correlation function (Eq. (1c)) is directly proportional to the concentration of the double-labeled species in the sample. By comparing the G(0) values, measured for free double-labeled DNA before it is mixed with the cationic liposomes, and after the same DNA is released from the lipoplexes, one can quantify the fraction of the double-labeled species in the released DNA.

For optimal correlation analysis, the concentration of fluorescent molecules usually has to be in the pico-to-nanomolar range. To satisfy this requirement, the lipoplexes were prepared using 5 pmol of double-labeled and 95 pmol of unlabeled 66-nt ds-DNA, and diluted to a final volume of ~400 μl. At this concentration of fluorescent species DNA-filled vesicles were not clearly recognizable by LSM, but were identified by monitoring fluorescent count rates in both channels of the FCCS setup. The FCCS measurements inside DOPS/DOPE/DOPC vesicles, containing released ds-DNA (Fig. 5A), demonstrated that the relative amplitude of the cross-correlation function for DNA, dissociated from the cationic complexes, remains at about the same level ($G(0)=0.028\pm0.002$) as was measured for free DNA in solution before preparation of the lipoplexes ($G(0)=0.03\pm0.002$, Fig. 5B). This result signifies that released DNA molecules, in bulk, have remained double-stranded. The other characteristic parameter, the diffusion time of cross-correlating species, also remains in a good agreement between the released and control DNA, Fig. 5A ($\tau_d=0.40\pm0.01$ ms) and B ($\tau_d=0.39\pm0.01$ ms). Another important observation is that for the released DNA (Fig. 5A,

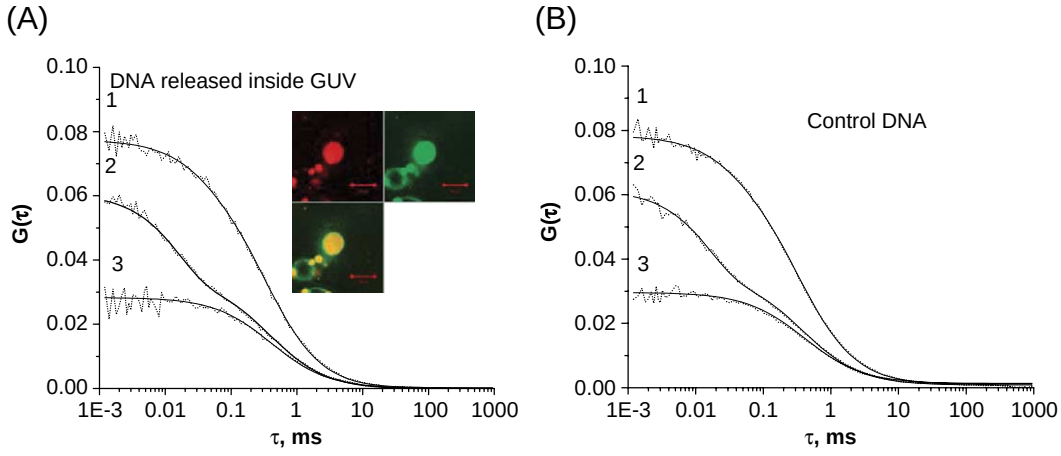

Fig. 5. Fluorescence correlation spectroscopy data for diffusion of 66-nt double-stranded DNA, labeled with Cy-5 and/or Alexa 488. (A) DNA released into DOPS/DOPE/DOPC (0.15/0.25/0.6) vesicles from DOTAP/DOPE lipoplexes (0.5/0.5), (B) control DNA diffusing in water. (1) an autocorrelation curve for Alexa 488 labeled molecules; (2) an autocorrelation curve for Cy-5 labeled molecules; (3) a cross-correlation curve for the double-labeled DNA molecules; in each plot experimental data are given by dotted lines, while solid lines represent fitted curves. The insert in (A) shows an illustrative example of the vesicle, filled with double-stranded DNA.

plots 1, 2) and for the control DNA (Fig. 5B, plots 1, 2) the auto-correlation curves of the fluorescent signals in the green and red channels separately have identical diffusion times. This provides evidence that released DNA is largely separated from the cationic lipids. One more detail, giving further support that released ds-DNA has dissociated from the carrier lipid, is the specific pronounced shoulder at the fast time slope of the auto-correlation curve for the red dye (curve 2, Fig. 5A). This fast range decay of the temporal correlation appears due to isomerization reactions of Cy-5 fluorophore, which is visualized as fast flickering of single dye molecules [57]. Such a bend in the fast time interval of the auto-correlation curve is a known brand mark of Cy-5 dye, and is also seen for the free DNA (curve 2, Fig. 5B). If a large number of fluorescent units diffuse in aggregates, as is the case of the cationic lipid-DNA complexes, fast flickering of single fluorophore would be statistically obscured and the pronounced shoulder in the curve would not be observed.

3.5. Real-time tracking of single lipoplex interaction with membranes

In earlier studies, the probable reason why DOTAP/DOPE-based lipoplexes exhibit higher efficiency of intracellular polynucleotide release was related to the propensity of these lipoplexes to fuse more rapidly upon binding the anionic vesicles [12]. At the same time, DOTAP/DOPC lipoplexes did not fuse for a longer time [12]. Newer findings reveal a more complicated picture of DOPE and DOPC activity as "helper" lipids, showing that under certain conditions DOTAP/DOPC-DNA lipoplexes could be as efficient as DOTAP/DOPE-DNA complexes [21]. To investigate the time course of lipoplex fusion with the target membrane in more detail, we monitor this process by the single particle tracking technique. In the SPT experiments, the GUVs were not labeled while the lipoplexes were prepared using 1 pmol of Cy-5 labeled ODN. The vesicles were prepared from DPPS/DOPE/DOPC (0.15/0.25/0.6) or DOPE/DOPC (0.4/0.6) lipid mixture. The lipoplexes were formed using DOTAP/DOPE or DOTAP/DOPC liposomes with varying amounts of helper lipids.

Fig. 6A shows a typical image of the lipoplexes on the GUV surface, immediately following the injection. At this stage, usually only a few complexes are seen attached to the membrane. This provides excellent observation conditions and allows us to clearly resolve movement of the individual lipoplexes. The subsequent images in Fig. 6B demonstrate that the lipoplexes did not burst rapidly upon binding to the membrane and remained compact, while undergoing lateral

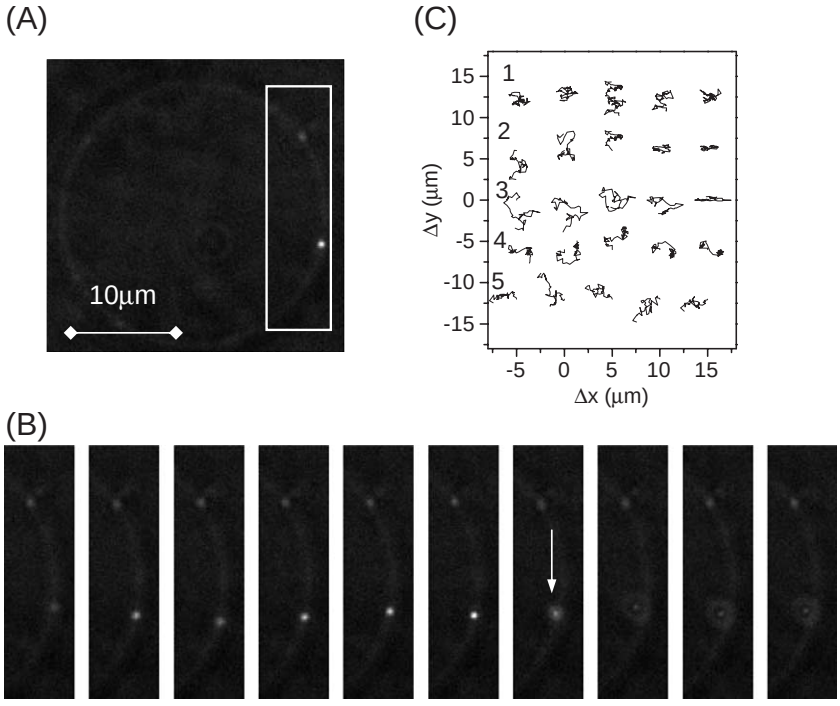

Fig. 6. Imaging and tracking of single lipoplex binding to the membrane. (A) an image of a non-labeled DPPS/DOPE/DOPC (0.15/0.25/0.6) vesicle, acquired immediately after injecting lipoplexes, showing single lipoplexes attached to the GUV membrane; (B) subsequent time series images for the segment of the vesicle in (A) demonstrating that bound lipoplexes undergo prolonged lateral movement before fusion; time lag between two subsequent frames is 40 ms. The non-labeled vesicles were injected with the DOTAP/DOPE lipoplexes (0.5/0.5 lipid mole fraction) containing 1 pmol of 66-nt Cy-5 labeled ODN; (C) typical trajectories of single lipoplexes on/in membrane bilayer. Each trajectory contains 50 steps with a time lag between two subsequent steps 40 ms. Horizontally aligned sets of trajectories correspond respectively to: (1) DOTAP/DOPE lipoplexes at 0.5/0.5 lipid mole fraction, (2) DOTAP/DOPE at 0.7/0.3 lipid mole fraction; (3) DOTAP/DOPE at 0.3/0.7 lipid mole fraction; (4) DOTAP/DOPC at 0.9/0.1 lipid mole fraction; (5) DOTAP/DOPC at 0.7/0.3 lipid mole fraction. The trajectories in each row from left to right are separated by increasing time intervals of 20 s. The arrow in (C) marks the particle, which moves out of the focus in the next frames.

motion on the lipid bilayer and lingering to fuse. This was observed both for DOTAP/DOPE and DOTAP/DOPC lipoplexes at various molar fractions of the "helper" lipids. Fig. 6C gives representative trajectories of different lipoplexes, obtained from analysis of approximately 60–90 particles for each type of lipoplex. Independent of the lipid formulation, the typical behavior of the lipoplexes was to diffuse as a compact particle on the membrane surface for up to ~60 s. Eventually, the particles showed a tendency of a constrained motion (last trajectories to the right in each horizontal row in Fig. 6) and spread, exhibiting diffuse fluorescence burst at the site of a previously seen distinct bright spot. This event was identified as lipoplex rupture and polynucleotide release. In contrast, when the particles remained compact but moved out of focus, it was possible to recognize them in the next frame (frames), as seen for the particle marked by the arrow in four last images in Fig. 6B. To avoid fast photo-bleaching of the fluorophores, the illumination intensity at the sample was adjusted such that the complexes did not photo-bleach for up to several minutes, as determined in the control experiments. The series of images in Fig. 7 shows a representative time course

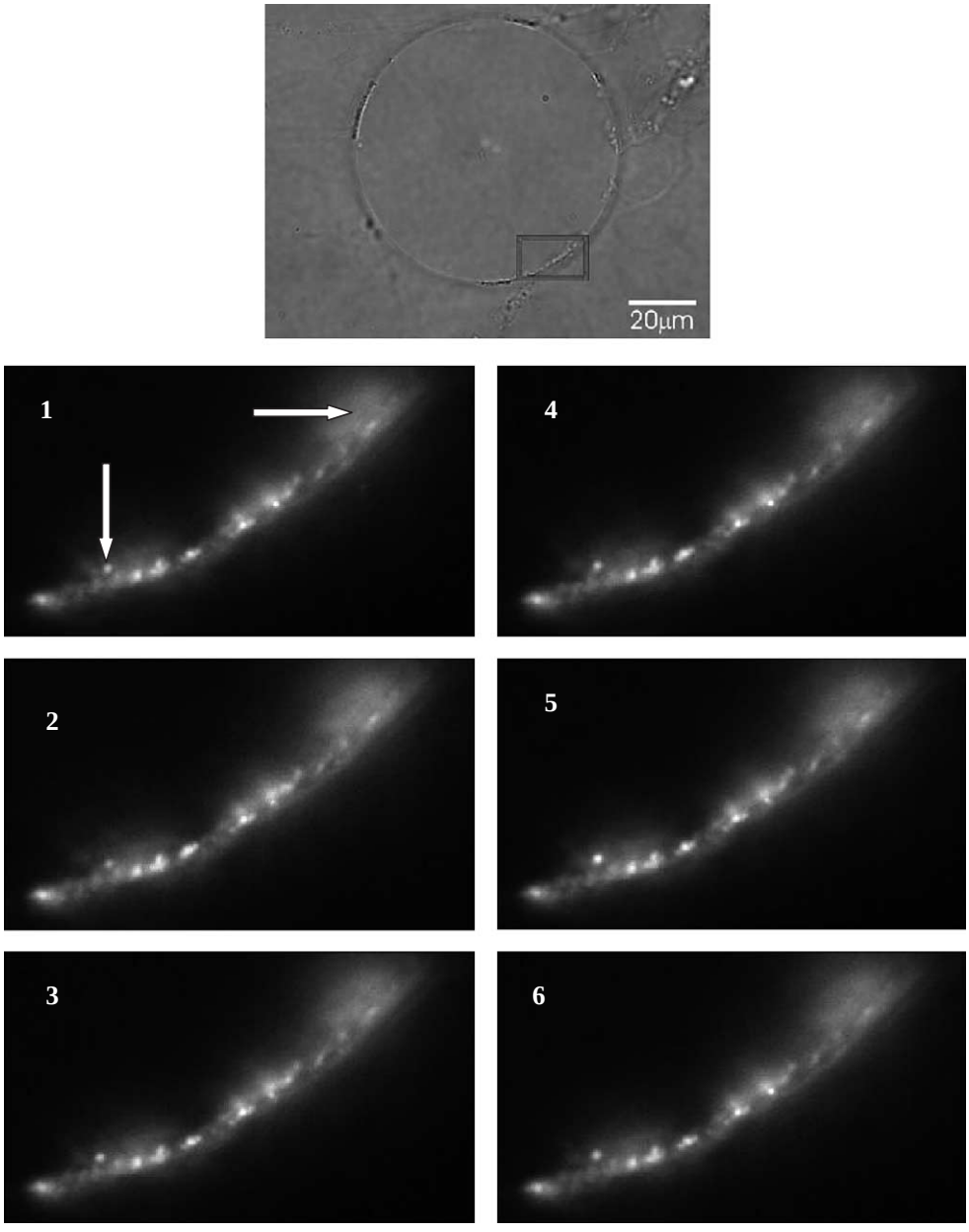

Fig. 7. Single particle imaging data for the non-labeled GUV sample approximately 10 min after lipoplex injection. (A) a phase contrast image of the vesicle; (B) subsequent time series frames for the fragment of the vesicle showing that bound lipoplexes, visualized by fluorescence of labeled polynucleotide, undergo lateral movement on/inside the membrane lipid bilayer and do not release DNA/ODN immediately upon binding but remain attached to the membrane for up to several minutes before fusion. The GUV sample was prepared using non-labeled DPPS/DOPE/DOPC (0.15/0.25/0.6) lipids and injected with the DOTAP/DOPC lipoplexes (0.9/0.1 lipid mole fraction) containing 10 pmol of 66-nt Cy-5 labeled ODN; a time lag between two subsequent frames is 15 s.

of lipoplex interaction with the membrane on the later stage, when more particles (DOTAP/DOPE lipoplexes, at 0.5/0.5 lipid molar fractions) attached to the membrane and polynucleotide release has been initiated. The blurring fluorescent spot on the vesicle's rim heading inward, seen in the upper right corner of the images, likely corresponds to DNA release inside the vesicle after fusion. At the same time, several distinct bright dots are observable as compact fluorescent spots in the lower left corner of the images for up to 1–3 min. This provides evidence that lipoplex fusion is rather a gradual effect determined by the kinetics of lipid mixing.

4. Discussion

The mechanism of DNA release from the cationic lipid carriers, which relies on the formation of the neutralized ion pair, assumes that presence of fully charged anionic phospholipids (such as PS) is a major requirement for lipoplex disruption and polynucleotide dissociation [31,32]. An important prerequisite for PS releasing activity is its translocation into the internal leaflet of an endosomal membrane, which would create the precondition for a closer contact with the entrapped cationic complexes. This putative event still remains a hypothetical concept. Although inside-to-outside phospholipid translocation during endocytosis in general, and during internalization of the cationic complexes in particular, would be consistent with various experimental observations [38–42], the probability and the mechanism of such a lipid "flip-flop" is undecided. Also, with the most accents on anionic PS, it is not clear what are the other phospholipid functions in the interaction with lipoplexes.

Using model membranes, we show directly that phospholipid formulations, typical of the endosomal membranes (DOPS/DOPE/SM/DOPC and/or DPPS/DOPE/SM/DOPC at 0.1/0.25/0.1/0.55) favor significant polynucleotide release from the lipoplexes. By varying the lipid content of the model membranes in the series of double and ternary mixtures of PS, PE, SM and PC and monitoring the extent of DNA release, we infer that polynucleotide release from lipoplexes is mediated primarily by PS and PE, while PC and SM are inert in this process. Additionally, the similar extent of DNA release for DOPS and DPPS containing membranes is the evidence that the acyl group of PS does not influence PS interaction with the cationic complexes.

Surprisingly, when anionic PS was excluded from the membranes and dual neutral composition PE/PC was probed (DOPE/DOPC, 0.25/0.75), the release remained at about the same high level as for PS/PC mixture. Apparently, this result indicates that the action of anionic PS lipids in DNA release is not unique and that neutral PE lipids can also be efficient stimulators of the release. To investigate this premise further, we probed the dual PE/PC membrane with the amount of PE increased up to 0.4 molar fraction (DOPE/DOPC, 0.4/0.6), which fully substitutes for PS in the ternary mixture PS/PE/PC. This dual PE/PC mixture showed a strong release. Taken together, the above observations signify that while PS is a strong agent in releasing DNA from the lipoplexes, its activity is enhanced by the presence of PE lipids in the membrane. At the same time, PE lipid by itself is an active promoter of lipoplex destabilization and DNA release.

Our data here about PS function in interaction with cationic lipid–DNA complexes support existing knowledge [31,32]. However, the new aspect revealed in our experiments is that the activity of anionic PS in polynucleotide release is strongly complemented by the action of neutral PE; and that PE is also equally potent to induce DNA release from the lipoplexes, without PS interference. By analyzing the earlier studies of others [31,32], which provided experimental evidence for the release mechanism suggesting a primary role of anionic PS in this process, we noticed that in the reported experiments PS was always included in the ternary mixtures with PE and PC. In particular, PS activity was probed using PS/DOPE/DOPC liposome composition at molar fractions 0.25/0.5/0.25, containing PE in the high amount. A dual PS/PC composition was not investigated, while the dual PE/PC composition as used in those experiments, contained PE in amounts equal or exceeding 50 mol%, i.e., DOPE/DOPC at 2:1 [31] or DOPE/DOPC at 1:1 [32]. It was reported that mixing DOPE/DOPC liposomes of such composition with the lipoplexes did not induce DNA release [31,32]. This observation is in contrast with our finding of strong DNA release by dual PE/PC mixture. A cause of the disagreement might be related to the specific amount of PE lipids included in the mixtures, investigated by us and by Szoka et al. [31,32]. Specifically, poorly hydrating lipids such as PE have a tendency to self-aggregate upon hydration. Lipid vesicles containing ~60 mol% of PE are particularly prone to create aggregates, which might form in the lipid suspension even after sonication (Preparation of liposomes, Technical Information, Avanti Polar Lipids, Inc., Alabaster, AL). Considering this fact, it is probable that PE/PC liposomes, containing more than 50 mol% of PE might be aggregated, which resulted in low releasing capability of such preparations as reported [31,32]. Therefore, it is likely that the releasing function of neutral PE lipid was overlooked in the previous experiments, and hence the key role in polynucleotide release was credited to anionic PS lipid alone.

In view of the new aspects of PE activity in polynucleotide release uncovered in our experiments, we suggest that the release mechanism emphasizing a key role of anionic PS in this process needs amendments. We propose a model, in which membrane aminophospholipids, PE and PS, are equally important promoters of lipoplex disassembly and polynucleotide release, and their actions toward release are complementary. It is likely that the extent of lipid scrambling at the very onset of lipoplex internalization in the endosomal compartment is a key factor determining the

efficiency of polynucleotide release. When cationic complexes bind a lipid bilayer, the whole reacting system becomes highly unstable and is driven from the equilibrium due to a combination of electrostatic and hydrophobic interactions involving the membrane lipids, the carrier lipids and polynucleotides. According to existing hypotheses, lipid mixing during lipoplex internalization likely stimulates PS flip-flop into the inner leaflet of the endosomal membrane, thereby creating conditions for efficient PS binding to the cationic lipids of the lipoplexes [31,32]. In this regard, the destabilizing activity of PE lipids at the onset of the complex entrapping into the endosomal compartment could be critical for the outcome of the lipoplex disruption and polynucleotide release. Due to its specific structure with a small hydrophilic head group, PE is inclined to bend the bilayer toward the side of its head group and thereby to form high curvature morphologies. Such an action would result in a strong destabilization of the contacting bilayers. Thus, if the extent of lipid mixing exceeds a certain critical level, the lipoplex could start releasing polynucleotide in the absence of anionic PS lipids, as observed here in the experiments with DOPE/DOPC target membranes. In endosomal compartments, the lipid mixing due to negative curvature-inclined PE together with electrostatic attraction of anionic PS to the cationic lipids would create strong destabilization of the system. Presumably, it could result in lateral as well as trans-leaflet lipid translocation, involving significant amounts of lipids. In such a case, a resulting variation of the ratio of the inner and outer areas between the two opposing monolayers would cause strong local deformations of the membrane [41]. In our experiments with giant vesicles, used here as enlarged models of endosomal membranes, we observed that lipoplex interaction with PE and/or PS containing membranes leads to strong DNA release while preserving the integrity of the contacting bilayers. In the real endosomal compartments with a higher curvature, though, this effect could possibly have different kinetics, and would lead not only to DNA release across the bilayer but may also result in endosome rupture.

The model which we put forward here, proposing that the extent of lipid mixing at the onset of lipoplex binding to the membrane is a predominant factor for triggering the lipoplex disruption and polynucleotide release, is consistent with our other new observations. Specifically, the formation of transient lipid domains, emerging in PS containing membranes at the early stage of lipoplex attachment to the membrane, likely reflects on lateral lipid translocation in the target bilayer. Based on the fact that this effect was observed only when PS was present in the membranes, we relate preferential lipoplex binding to local re-distribution of PS lipids. Attachment of a strongly positively charged complex to the membrane causes additional anionic lipids to move to this site, thereby enhancing lipid mixing and destabilizing the interacting parts. The transitory character of these domains, which gradually dispersed as more lipoplexes attached to the membrane and/or active polynucleotide release has been triggered, might signify that the strongest destabilization of the system occurs at the very first moments of interaction, and the influx of additional anionic lipids to the sites of lipoplex binding reflects on the response of the destabilized lipid bilayer. Modeling real biological membranes by liposomes (including GUVs) has the unavoidable shortcoming that it is problematic to reproduce a real asymmetrical transmembrane phospholipids distribution in liposomes [58,59]. Thus, in our experiments it was possible to observe explicitly only the lateral movement of the lipids in the bilayer, with no direct evidence of the trans-leaflet lipid translocation. However, indirect evidence that possible trans-leaflet lipid translocation could also be involved during lipoplex binding to the membrane is given by extensive membrane vesiculation in the sites of binding. As described earlier by others, abundant membrane vesiculation could sing of induced membrane lipid asymmetry as the disturbed lipid bilayer gains a new equilibrium state via producing budding-vesicle shapes [59]. In addition, our observations that the average time interval needed for the lipoplex fusion is approximately 1–2 min (as revealed by tracking single lipoplexes on the GUV surface) provide further support to the idea that the extent of lipid mixing is a key factor for starting the release.

Another important aspect of DNA release which we report here, is that double-stranded DNA remains a duplex in this process. As self-assembling of discrete particles from cationic liposomes and DNA involves a major rearrangement of each component to form a compact ordered unit, the DNA structure was shown to undergo significant changes during its condensation into the lipoplex [60–62]. As was demonstrated by probing DNA conformational modifications within the cationic complexes using the potassium permanganate ($KMnO_4$) assay [62,63], double-stranded DNA was partially melted during formation of the lipoplexes, and showed appearance of single-stranded regions. By monitoring diffusion of double-labeled DNA molecules, our FCCS data clearly demonstrate that for short polynucleotides two complimentary DNA strands remain attached and do not come apart upon release from the lipoplexes. However, our noninvasive assay could not be applied to detect appearance of partial DNA melting.

While multiple observations have demonstrated that DOTAP/DOPE lipoplexes transfer DNA more efficiently than pure DOTAP lipoplexes and, in general, more efficiently than DOTAP/DOPC lipoplexes [12,14,45–47], it remains unclear why. Here, we observe more complex behavior of DOTAP/DOPE and DOTAP/DOPC lipoplexes. Specifically, release from DOTAP/DOPE complexes was significant and rather independent of the fraction of the helper lipids, while DOTAP/DOPC lipoplexes were efficient in releasing DNA only with a small fraction of DOPC included. These data are in agreement with the cellular observations of others, demonstrating that transfection efficiency of DOTAP/DOPC complexes at low DOPC content can match the efficiency of DOTAP/DOPE com-

plexes [21]. The probable reason for this is a higher membrane charge density of DOTAP/DOPC lipoplexes at a lower fraction of DOPC [21]. Though our data are rather confirmatory in this case, the important inference is that using a model system of giant unilamellar vesicles provides a feasible assay to probe the transfection potential of newly designed cationic liposome carriers.

In the current work, we report results obtained with the lipoplexes prepared from short single and double strand polynucleotides. Considering the similarity of long plasmid DNA and short ODN lipoplexes behavior during the release as reported earlier by others [31,32], it is likely that the events observed here will take place also for the plasmid lipoplexes. However, conclusive demonstration of this aspect will have to be probed by performing similar experiments with long DNA, which were beyond the goals of this study.

In summary, we conclude that phospholipid composition of the endosomal membranes is predisposed for inducing significant polynucleotide release from the lipoplexes, and that PE and PS are equally significant for this process, while PC and SM are inert. Amending the existing understanding of release mechanisms, we propose that extensive lipid mixing between the lipoplexes and contacting membrane as well as inside the target bilayer at the onset of lipoplex binding is a determining factor for release; and that negative curvature neutral PE lipids are similar in release efficiency to anionic PS lipids. The question remains as to why endocytosis is required for mediating nucleotide release from the lipid carriers, considering that the phospholipid composition of endosomal membranes, being predisposed to disrupt lipoplexes, is similar to the composition of the cytoplasmic leaflet of the plasma membrane. The experiments reported here were not designed to address this question, and we only attempted to gain deeper insights into the mechanisms by which polynucleotides can escape from the endosomal compartments and get rid of the cationic lipids. The endocytosis-mediated path for lipoplex intracellular entry was accepted here as the best experimentally confirmed model [23–28]. A probability of trans-leaflet lipid mixing and higher curvature of endosomal membranes might be potential causes for endocytosis requirements, although it would be speculative to suggest any models in this regard in our current work.

Acknowledgements

This study was supported in part by Research Fellowship from Alexander von Humboldt Foundation to S.B. and also by a Research Grant from Volkswagen Foundation to P.S.

We thank all members of “Biofuture” group in MPI for Biophysical Chemistry, Goettingen for interesting and stimulating discussions. S.B. is thankful to Dr. Ruthild Winkler-Oswatitsch for general support throughout this work.

References

[1] T.M. Allen, P.R. Cullis, Drug delivery systems: entering the mainstream, Science 303 (2004) 1818–1822.
[2] L. Scherer, J. Rossi, Approaches for the sequence specific knockdown of mRNA, Nat. Biotechnol. 21 (2003) 1457–1465.
[3] A.S. Ulrich, Biophysical aspects of using liposomes as delivery vehicles, Biosci. Rep. 22 (2002) 129–150.
[4] M.C. Pedroso de Lima, S. Simoes, P. Pires, H. Faneca, N. Duzgunes, Cationic lipid–DNA complexes in gene delivery: from biophysics to biological applications, Adv. Drug Deliv. Rev. 47 (2001) 277–294.
[5] S. Chesnoy, L. Huang, Structure and function of lipid–DNA complexes for gene delivery, Annu. Rev. Biophys. Biomol. Struct. 2 (2000) 27–47.
[6] M.B. Bally, P. Harvie, F.M. Wong, S. Kong, E.K. Wasan, D.L. Reimer, Biological barriers to cellular delivery of lipid-based DNA carriers, Adv. Drug. Deliv. Rev. 38 (1999) 291–315.
[7] N. Maurer, A. Mori, L. Palmer, M.A. Monck, K.W. Mok, B. Mui, Q.F. Akhong, P.R. Cullis, Lipid-based systems for the intracellular delivery of genetic drugs, Mol. Membr. Biol. 16 (1999) 129–140.
[8] H. Gershon, R. Ghirlando, S.B. Guttman, A. Minsky, Mode of formation and structural features of DNA-cationic liposome complexes used for transfection, Biochemistry 32 (1993) 7143–7151.
[9] F.M.P. Wong, D.L Reimer, M.B. Bally, Cationic lipid binding to DNA: characterization of complex formation, Biochemistry 35 (1996) 5763–5776.
[10] S.J. Eastman, C. Sigel, J. Tousignant, A.E. Smith, S.H. Cheng, R.K. Scheule, Biophysical characterization of cationic lipid: DNA complexes, Biochim. Biophys. Acta 1325 (1997) 41–62.
[11] Y.-P. Zhang, D.L. Reimer, G. Zhang, P.H. Lee, M.B. Bally, Self-assembling DNA–Lipid particles for gene transfer, Pharm. Res. 14 (1997) 190–196.
[12] I. Koltover, T. Salditt, J.O. Raedler, C.R. Safinya, An inverted hexagonal phase of cationic liposome–DNA complexes related to DNA release and delivery, Science 281 (1998) 78–81.
[13] I. Koltover, T. Salditt, C.R. Safinya, Phase diagram, stability, and overcharging of lamellar cationic lipid–DNA self-assembled complexes, Biophys. J. 77 (1999) 915–924.
[14] Y. Xu, S.W. Hui, P. Frederik, F.C. Szoka, Physicochemical characterization and purification of cationic lipoplexes, Biophys. J. 77 (1999) 341–353.
[15] V. Oberle, U. Bakowsky, I.S. Zuhorn, D. Hoekstra, Lipoplex formation under equilibrium conditions reveals a three-step mechanism, Biophys. J. 79 (2000) 1447–1454.
[16] I. Koltover, K. Wagner, C.R. Safinya, DNA condensation in two dimensions, Proc. Natl. Acad. Sci. U. S. A. 97 (2000) 14046–14051.
[17] M.E. Ferrari, D. Rusalov, J. Enas, C.J. Wheeler, Trends in lipoplex physical properties dependent on cationic lipid structure, vehicle and complexation procedure do not correlate with biological activity, Nucleic Acids Res. 29 (2001) 1539–1548.
[18] D. Simberg, D. Danino, Y. Talmon, A. Minsky, M.E. Ferrari, C.J. Wheeler, Y. Barenholz, Phase behavior, DNA ordering, and size instability of cationic lipoplexes, J. Biol. Chem. 276 (2001) 47453–47459.
[19] J. Smisterová, A. Wagenaar, M.C.A. Stuart, E. Polushkin, G. Brinke, R. Hulst, J.B.F.N. Engberts, D. Hoekstra, Molecular shape of the cationic lipid controls the structure of cationic lipid/dioleoylphosphatidylethanolamine–DNA complexes and the efficiency of gene delivery, J. Biol. Chem. 276 (2001) 47615–47622.
[20] C. Madeira, L.M.S. Loura, R.M. Aires-Barros, A. Fedorov, M. Prieto, Characterization of DNA/Lipid complexes by fluorescence resonance energy transfer, Biophys. J. 85 (2003) 3106–3119.
[21] A.J. Lin, N.L. Slack, A. Ahmad, C.X. George, C.E. Samuel, C.R. Safinya, Three-dimensional imaging of lipid gene-carriers: membrane charge density controls universal transfection behavior in lamellar cationic liposome–DNA complexes, Biophys. J. 84 (2003) 3307–3316.

[22] S. Weisman, D. Hirsch-Lerner, Y. Barenholz, Y. Talmon, Nanostructure of cationic lipid–oligonucleotide complexes, Biophys. J. 87 (2004) 609–614.
[23] X. Zhou, L. Huang, DNA transfection mediated by cationic liposomes containing lipopolylysine: characterization and mechanism of action, Biochim. Biophys. Acta 1189 (1994) 195–203.
[24] I. Wrobel, D. Collins, Fusion of cationic liposomes with mammalian cells occurs after endocytosis, Biochim. Biophys. Acta 1235 (1995) 296–304.
[25] D.S. Friend, D. Papahadjopoulos, R.J. Debs, Endocytosis and intracellular processing accompanying transfection mediated by cationic liposomes, Biochim. Biophys. Acta 1278 (1996) 41–50.
[26] O. Zelphati, F.C. Szoka, Intracellular distribution and mechanism of delivery of oligonucleotides mediated by cationic lipids, Pharm. Res. 13 (1996) 1367–1372.
[27] I.S. Zuhorn, R. Kalicharan, D. Hoekstra, Lipoplex-mediated transfection of mammalian cells occurs through the cholesterol-dependent clathrin-mediated pathway of endocytosis, J. Biol. Chem. 277 (2002) 18021–18028.
[28] I.S. Zuhorn, D. Hoekstra, On the mechanism of cationic amphiphile-mediated transfection. To fuse or not to fuse: is that the question? J. Membr. Biol. 189 (2002) 167–179.
[29] R. Urade, Y. Hayashi, M. Kito, Endosomes differ from plasma membrane in the phospholipid molecular species composition, Biochim. Biophys. Acta 946 (1988) 151–163.
[30] T. Kobayashi, M.H. Beuchat, J. Chevallier, A. Makino, N. Mayran, J.M. Escola, C. Lebrand, P. Cosson, J. Gruenberg, Separation and characterization of late endosomal membrane domains, J. Biol. Chem. 277 (2002) 32157–32164.
[31] O. Zelphati, F.C. Szoka, Mechanism of oligonucleotide release from cationic liposomes, Proc. Natl. Acad. Sci. U. S. A. 93 (1996) 11493–11498.
[32] Y. Xu, F.C. Szoka, Mechanism of DNA release from cationic liposome/DNA complexes used in cell transfection, Biochemistry 35 (1996) 5616–5623.
[33] C. Moreau, J.C. Sulpice, P.F. Devaux, A. Zachowski, Drug-induced transmembrane lipid scrambling in erythrocytes and in liposomes requires the presence of polyanionic phospholipids, Mol. Membr. Biol. 14 (1997) 5–12.
[34] M. Seigneuret, P.F. Devaux, ATP-dependent asymmetric distribution of spin-labeled phospholipids in the erythrocyte membrane; relation to shape change, Proc. Natl. Acad. Sci. U. S. A. 81 (1984) 3751–3755.
[35] D.L. Daleke, W.H. Huestis, Incorporation and translocation of aminophospholipids in human erythrocytes, Biochemistry 24 (1985) 5406–5416.
[36] P.F. Devaux, A. Zachowski, E. Favre, P. Fellmann, S. Cribier, D. Geldwerth, P. Hervé, M. Seigneuret, Translocation énergie dépendante des amino-phospholipides dans la membrane des globules rouges, Biochimie 6 (1986) 383–393.
[37] P.F. Devaux, Static and dynamic lipid asymmetry in cell membranes, Biochemistry 30 (1991) 1163–1173.
[38] T. Pomorski, P. Müller, B. Zimmermann, K. Burger, P.F. Devaux, A. Herrmann, Transbilayer movement of fluorescent and spinlabeled phospholipids in the plasma membrane of human fibroblasts: a quantitative approach, J. Cell Sci. 109 (1996) 687–698.
[39] U. Marx, T. Polawkowski, T. Pomorski, C. Lang, H. Nelson, N. Nelson, A. Herrmann, Rapid transbilayer movement of fluorescent phospholipid analogues in the plasma membrane of endocytosis-deficient cells does not require the Drs2 protein, Eur. J. Biochem. 263 (1999) 254–263.
[40] X. Tang, M.S. Halleck, R.A. Schlegel, P. Williamson, A subfamily of P-type ATPase with aminophospholipid transporting activity, Science 272 (1996) 1495–1497.
[41] P.F. Devaux, Is lipid translocation involved during endo- and exocytosis? Biochimie 82 (2000) 497–509.
[42] R.D. Kornberg, H.M. Mc Connell, Inside–outside translocation of phospholipids in vesicle membranes, Biochemistry 10 (1971) 1111–1120.
[43] F.M.P. Wong, D.L. Reimer, M.B. Bally, Cationic lipid binding to DNA: characterization of complex formation, Biochemistry 35 (1996) 5763–5776.
[44] P. Harvie, F.M.P. Wong, M.B. Bally, Characterization of lipid DNA interactions: I. Destabilization of bound lipids and DNA dissociation, Biophys. J. 75 (1998) 1040–1051.
[45] F.M.P. Wong, P. Harvie, Y.P. Zhang, E.C. Ramsay, M.B. Bally, Phosphatidylethanolamine mediated destabilization of lipid-based pDNA delivery systems, Int. J. Pharm. 255 (2003) 117–127.
[46] H. Farhood, N. Serbina, L. Huang, The role of dioleoyl phosphatidylethanolamine in cationic liposome mediated gene transfer, Biochim. Biophys. Acta 1235 (1995) 289–295.
[47] S. Hui, M. Langner, Y. Zhao, P. Ross, E. Hurley, K. Chan, The role of helper lipids in cationic liposome-mediated gene transfer, Biophys. J. 71 (1996) 590–599.
[48] U. Kettling, A. Koltermann, P. Schwille, M. Eigen, Real time enzyme kinetics of restriction endonuclease EcoRI monitored by dual-color fluorescence cross-correlation spectroscopy, Proc. Natl. Acad. Sci. U. S. A. 95 (1998) 11420–14116.
[49] M.I. Angelova, D.S. Dimitrov, Liposome electroformation, Faraday Discuss. Chem. Soc. 81 (1986) 303–308.
[50] D.S. Dimitrov, M.I. Angelova, Lipid swelling and liposome electroformation mediated by electric fields, Bioelectrochem. Bioenerg. 19 (1988) 323–333.
[51] N. Kahya, D. Scherfeld, K. Bacia, B. Poolman, P. Schwille, Probing lipid mobility of raft-exhibiting model membranes by fluorescence correlation spectroscopy, J. Biol. Chem. 278 (2003) 28109–28115.
[52] U. Kubitscheck, O. Kouckmann, T. Kues, R. Peters, Imaging and tracking of single GFP molecules in solution, Biophys. J. 78 (2000) 2170–2179.
[53] A.L. Bailey, P.R. Cullis, Membrane fusion with cationic liposomes: effects of target membrane lipid composition, Biochemistry 36 (1997) 1628–1634.
[54] T.S. Blom, M. Koivusalo, E. Kuismanen, R. Kostiainen, P. Somerharju, E. Ikonen, Mass spectrometric analysis reveals an increase in plasma membrane polyunsaturated phospholipid species upon cellular cholesterol loading, Biochemistry 40 (2001) 14635–14644.
[55] C. Dietrich, L.A. Bagatolli, Z.N. Volovyk, N.L Thompson, M. Levi, K. Jacobson, E. Gratton, Lipid rafts reconstituted in model membranes, Biophys. J. 80 (2001) 1417–1428.
[56] A. Koltermann, U. Kettling, J. Stephan, M. Rabach, T. Winkler, M. Eigen, Applications of dual-color confocal fluorescence spectroscopy in biotechnology, in: R. Rigler (Ed.), Single Molecule Spectroscopy (Nobel Conference Lectures), Springer, New York, 2001, pp. 211–226.
[57] J. Widengren, P. Schwille, Characterization of photo-induced isomerization and back-isomerization of the cyanine dye Cy-5 by fluorescence correlation spectroscopy, J. Chem. Phys. 104 (2000) 6416–6428.
[58] J.A.F Op Den Kamp, Lipid asymmetry in membranes, Annu. Rev. Biochem. 48 (1979) 47–71.
[59] M. Trayikia, D.E. Warschawski, O. Lambert, J.L. Rigaudand, P.F. Devaux, Asymmetrical membranes and surface tension, Biophys. J. 83 (2002) 1443–1454.
[60] V.A. Bloomfield, DNA condensation, Curr. Opin. Struct. Biol. 6 (1996) 334–341.
[61] C.S Braun, G.S. Jas, S. Choosakoonkriang, G.S. Koe, J.G. Smith, C.R. Middaugh, The structure of DNA within cationic lipid/DNA complexes, Biophys. J. 84 (2003) 1114–1123.
[62] T.K. Prasad, V. Gopal, Rao N. Madhusudhana, Cationic lipids and cationic ligands induce DNA helix denaturation: detection of single stranded regions by $KMnO_4$ probing, FEBS Lett. 552 (2003) 199–206.
[63] S. Sasse-Dwight, J.D. Gralla, KMnO4 as a probe for lac promoter DNA melting and mechanism in vivo, J. Biol. Chem. 264 (1989) 8074–8081.